Available online at www.sciencedirect.com

ScienceDirect

Biochimica et Biophysica Acta 1768 (2007) 3001–3011

Biochimica et Biophysica Acta BBA

www.elsevier.com/locate/bbamem

Structural analysis of pituitary adenylate cyclase-activating polypeptides bound to phospholipid membranes by magic angle spinning solid-state NMR

Nobuyasu Komi [a], Kayo Okawa [a], Yukihiro Tateishi [b], Masahiro Shirakawa [b], Toshimichi Fujiwara [a], Hideo Akutsu [a,*]

[a] *Institute for Protein Research, Osaka University, 3-2 Yamadaoka, Suita 565-0871, Japan*
[b] *Kyoto University, Kyoto-Daigaku Katsura, Nishikyo-ku, Kyoto 615-8510, Japan*

Received 12 July 2007; received in revised form 6 October 2007; accepted 10 October 2007
Available online 23 October 2007

Abstract

PACAP (pituitary adenylate cyclase-activating polypeptide) is a member of the VIP/secretin/glucagon family, which includes the ligands of class II G-protein coupled receptors. Since the recognition of PACAP by the receptor may involve the binding of PACAP to membranes, its membrane-bound structure should be important. We have carried out structural analysis of uniformly ^{13}C,^{15}N labeled PACAP27 and its C-terminal truncated form PACAP(1–21)NH_2 (PACAP21) bound to membranes with high resolution solid-state NMR. Phosphatidylcholine bilayers and phosphatidylcholine/phosphatidylglycerol bilayers were used for PACAP27 and PACAP21, respectively. Most backbone signals were assigned for PACAP27 and PACAP21. TALOS analysis revealed that both peptides take on extended conformations on the membranes. Dilution of PACAP21 did not change the conformation of the major part. Selective polarization transfer experiment confirmed that PACAP27 is interacting with the membranes. It was concluded that the interaction of PACAP with the membrane surface causes their extended conformation. PACAP27 is reported to take an α-helical conformation in dodecylphosphocholine micelles and membrane-binding peptides usually take similar conformations in micelles and in membranes. Therefore, the property of PACAP27 changing its conformation in response to its environment is unique. Its conformational flexibility may be associated with its wide variety of functions.

Keywords: Pituitary hormone; PACAP27; Membrane-bound peptide; Isotope-labeling; NMR signal assignment; Extended conformation

1. Introduction

PACAP (pituitary adenylate cyclase-activating polypeptide) is a hormone peptide classified into VIP/secretin/glucagon family, which are ligands of class II G-protein coupled receptors. This peptide was first isolated from ovine hypothalamus, which directly stimulates the release of several pituitary hormones. Two forms of PACAP, which are composed of 27 and 38 amino acid residues, have been found, and are called PACAP27 and PACAP38, respectively. The amino acid sequence of the former is identical to that of the N-terminal 27 residues of the latter. PACAP is evolutionally conserved in vertebrates. The primary structure of PACAP38 has been totally conserved among human [1], sheep [2], rat [3], and mouse [4]. The sequences of PACAP38 and PACAP27 are shown below along with a C-terminal truncated derivative, PACAP21.

PACAP38 HSDGIFTDSYSRYRKQMAVKKYLAAVLGK-RYKQRVKNK-NH_2
PACAP27 HSDGIFTDSYSRYRKQMAVKKYLAAVL-NH_2
PACAP21 HSDGIFTDSYSRYRKQMAVKK-NH_2

The sequence of PACAP has been determined for several non-mammalian vertebrates and invertebrates, including chicken *Galus domesticus* [5], frog *Rana ridibunda* [6], salmon

Abbreviations: CP, cross-polarization; DARR, dipolar assisted rotational resonance; DMPC, 1,2-dimyristoyl-*sn*-glycero-3-phosphocholine; DPPC, 1,2-dipalmitoyl-*sn*-glycero-3-phosphocholine; DPPG, 1,2-dipalmitoyl-*sn*-glycero-3-phosphatidylglycerol; DSS, 2,2-dimethylsilapenatane-5-sulfonic acid; LGCP, Lee–Goldburg cross polarization; PACAP, pituitary adenylate cyclase-activating polypeptide; RFDR, radio-frequency-driven recoupling; SPC-5, five-step super phase cycle; TPPM, two-pulse phase modulation; trNOE, transferred nuclear Overhauser effect; VIP, vasoactive intestinal polypeptide

* Corresponding author. Fax: +81 6 6872 8219.
E-mail address: akutsu@protein.osaka-u.ac.jp (H. Akutsu).

0005-2736/$ - see front matter © 2007 Elsevier B.V. All rights reserved.
doi:10.1016/j.bbamem.2007.10.015

Oncorhynchus nerka [7], catfish *Clarias macrocephalus* [8] and tunicate *Chelyosoma productum* [9]. There is 96% sequence identity between human and tunicate PACAP27 [9]. These facts suggest that there have been a high evolutionary pressure to conserve the PACAP sequence.

In view of the sequence homology, the mechanism underlying the binding of PACAP to its receptor should be fundamentally conserved as well. The PACAP receptors are classified into 3 subtypes, i.e. PAC1, VPAC1 and VPAC2. PAC1 is involved in several neurotransduction systems, and is found in brain areas, including the hypothalamus. Therefore, PACAP might be working as neurotransmitter/neuromodulator and hypophysiotropic neurohormone regulator [10–12]. PACAP receptors are located not only in the brain, but also in peripheral tissues. VPAC1 and VPAC2, which serve as high affinity receptors for both PACAP and VIP, are primarily coupled with adenylate cyclase in the human muscle, heart, lung, kidney, stomach, testis, pancreas, and liver. This peptide acts as a blood pressure depressor [13], a smooth muscle relaxing factor [14], a promotion factor of insulin release from the pancreatic β-cell, and so on [15]. Thus, PACAP plays important roles in various physiological regulation systems.

The tertiary structures of PACAP21 bound to the PAC1 receptor and PACAP27 in dodecylphosphocholine (DPC) micelles were determined by transferred nuclear Overhauser effect (trNOE) and steady-state NOE, respectively [16]. The structure of micelle-bound PACAP27 comprises a long α-helix (residues 5–27) flanked by a disordered N-terminal tail (residues 1–4). In the case of the receptor-bound PACAP21 structure, however, an extended N-terminal tail (residues 1–2) is followed by consecutive β-turns (residues 3–7) and an α-helix (residues 8–21). A two-step model for the ligand targeting to the receptor through the membrane surface was proposed on the basis of the obtained conformations. Recently, the solution structure of N-terminally truncated PACAP38 (residue 6–38) binding to the extracellular domain of the PAC1 receptor was determined by NMR [17]. The peptide takes on a curved α-helix in the receptor.

Since the recognition of PACAP by the receptor and the following signal transduction take place in the membrane systems and a model for the recognition mechanism involves membrane-binding of PACAP, it is important to know the conformations of PACAP27 bound to membranes. For the analysis of the membrane-bound peptide, solid-state NMR is one of the most suitable methods. We have actually shown that this is a promising method through the structural analysis of a G-protein activating peptide, mastoparan X [18,19] and H^+-ATPsynthase subunit c [20]. Conformational studies of other membrane-bound peptides have been reported as well [21]. The results reported so far have revealed that many of them take on α-helices in their major parts. Usually, it is not easy to obtain uniformly isotope labeled peptides for NMR analysis. We have developed an efficient expression system for PACAP peptides. Then, the structural analysis of membrane-bound PACAP peptides by solid-state CP/MAS NMR has been carried out in this work. The result has shown that the conformations of the membrane-bound peptides are different from that of the micelle-bound one and PACAP peptides assume different conformations depending on the interacting partners.

2. Materials and methods

2.1. Peptide expression and purification

A pET21b vector was used to clone a gene of the fusion protein of thioredoxin (Trx) and PACAP21-Gly or PACAP27-Gly with an N-terminal 6His-tag [22]. It was introduced into competent *Escherichia coli* (*E. coli*) BL21 (DE3) (Novagen, Madison, WI, USA) and expressed under the control of *lac* promoter. A single colony was inoculated into 5 ml of LB medium containing ampicillin (50 μg/ml) and it was incubated for 3–5 h at 37 °C. When OD_{660} became 0.5, 1 ml of the culture was inoculated into 500 ml of CHL medium (CHLORELLA Industry Co., Tokyo, Japan) with ampicillin (50 μg/ml) in a 2-l baffled flask, which was incubated for about 4 h at 37 °C with a shaking rate at 120 rpm. At 0.2 $OD_{660,}$ the temperature was adjusted to 30 °C. At 0.5 OD_{660}, isopropylthio-β-D-galactoside (IPTG) was added (final 0.8 mM) for induction. The cells were further incubated for 6 h (up to about 1 OD_{660}) and harvested. The cell suspension was sonicated for 10 min (2 min interval per min) at 4 °C and was centrifuged for 20 min at 20000 rpm. The supernatant was applied to a DEAE column. Then, the fusion protein was purified by Ni-NTA superflow (Qiagen, Valencia, CA, USA) affinity column chromatography at 4 °C and was concentrated. For isotope-labeling, 1 ml culture at OD_{660}=0.5 was centrifuged at 6000 rpm. The pellet was suspended with 0.1 ml of a 0.9% NaCl solution, and added to 500 ml of a ^{13}C,^{15}N labeled CHL medium.

For cleavage of the fusion protein, Factor Xa (New England Biolabs, Beverly, MA, USA) was added at 0.25% (w/w) of the substrate in a 100 mM NaCl, 50 mM Tris–HCl buffer, pH 7.4. The substrate concentration was about 0.6 mM. The reaction mixture was incubated for 3 h at 4 °C. The Factor Xa was removed with a Sep-Pak C18 environmental cartridge (Waters, Milford, MA, USA). The PACAP21-Gly or PACAP27-Gly was eluted with acetonitrile solution (50–70%) containing 0.05% (v/v) TFA, then purified by reverse-phase HPLC (Gilson, Middleton, WI, USA) with a Wakosil 5C18 column (Wako Pure Chemical Industries, Ltd, Osaka, Japan) and a linear water/acetonitrile gradient containing 0.05% TFA.

C-terminal amidation of the obtained peptide was achieved by the oxidation of its terminal Gly residue with peptidylglycine α-amidating enzyme [23]. The purified PACAP was obtained with the HPLC again. The purities of these peptides were confirmed by Tricine-SDS-PAGE and mass spectrometry using a matrix-assisted laser desorption ionization time-of-flight (MALDI-TOF) mass spectrometer (Autoflex, Bruker Daltonics, Germany). Peptidylglycine amidating monoxygenase was purchased from Wako Pure Chemical Industries, Ltd (Japan).

2.2. Preparation of membrane-bound peptides

Multilamellar liposomes were prepared by a freeze-and-thaw treatment. For PACAP21, deuterated 1,2-dipalmitoyl-*sn*-glycero-3-phosphocholine-d_{62} (DPPC, 98% ^2H) and deuterated 1,2-dipalmitoyl-*sn*-glycero-3-phosphoglycerol-d_{62} (DPPG, 98% ^2H) were used to prepare liposomes. They were dissolved in chloroform/methanol (1:1, v/v), and then the solution was dried to a film by evaporator. The ratio of DPPC to DPPG was 4 to 1 (mol/mol). It was further dried under high vacuum to remove all trace of organic solvent. The dried film was suspended in ultrapure water. The final concentration of the suspension was 10 mg/ml. The lipid suspension was subjected to typically ten freeze/thaw cycles. For PACAP27, deuterated 1,2-dimyristoyl-*sn*-glycero-3-phosphocholine-d_{54} (DMPC, 98% ^2H) was used as the phospholipid. Then, the peptide was added to the liposome suspension (lipid/PACAP21=36 and 360, and lipid/PACAP27=20 mol/mol), followed by about ten freeze/thaw cycles. The supernatant was removed by centrifugation at 30000 g for 30 min. DMPC-d_{54}, DPPC-d_{62}, and DPPG-d_{62} were purchased from Cambridge Isotope Laboratories Inc. (Andover, MA, USA). The liposomes with peptides were once dried and then hydrolyzed under 32% relative humidity. The samples of PACAP21 (3.8 mg) and PACAP27 (4 mg) were transferred to 4 mm and 3.2 mm rotors, respectively.

2.3. Solid-state NMR spectroscopy

NMR measurements were performed with Varian Infinity-plus 500, 600 and 700 spectrometers (Palo Alto, CA, USA) operating at 11.74, 14.09 and 16.44 T static magnetic fields, respectively. Broadband double and triple resonance MAS probes for the sample rotors with 3.2 and 4 mm diameters were used. The

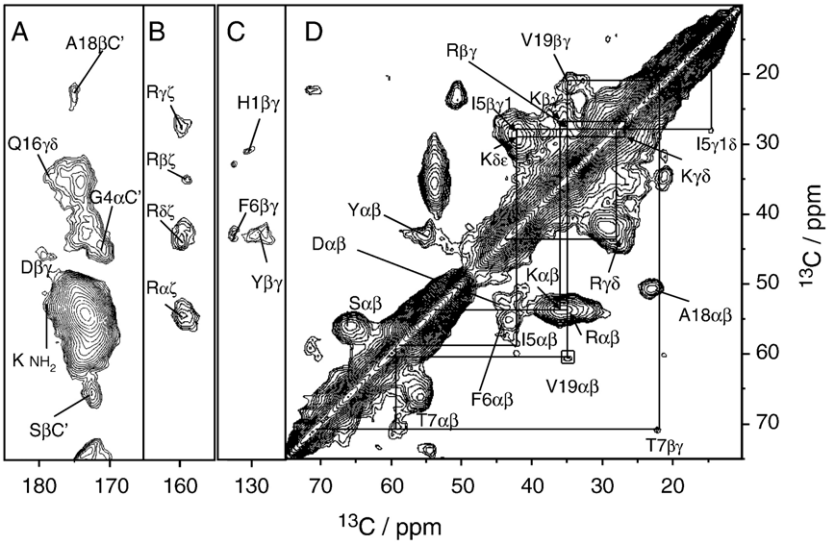

Fig. 1. 2D ^{13}C–^{13}C correlation DARR spectra of membrane-bound [U–^{13}C, ^{15}N] PACAP21 at 11.74 T and 223 K. DARR mixing time, 9 ms for A, C and D, and 200 ms for B; number of acquisition, 64 for each FID; and MAS frequency (ω_R) = 12.5 kHz. (A) aliphatic-carbonyl carbon correlation, (B) Arg and Tyr region, (C) Cβ-aromatic Cγ correlation, and (D) aliphatic carbon correlation. The side-chain connectivity was indicated with solid lines for Ile, Thr, Val, Arg, and Lys. Sensitivity is enhanced in the squared region.

MAS frequency was 12.5–16 kHz. The sample temperature was set at 193–273 K. The ^{1}H radio frequency (RF) amplitude was 70 kHz for TPPM decoupling [24]. Lee–Goldburg cross-polarization experiment [25], two-dimensional ^{13}C homonuclear correlation experiment RFDR [26,27], SPC-5 [28] and DARR [29,30] were recorded with standard pulse sequences. The ^{1}H RF amplitude for DARR was 12.5 kHz. Heteronuclear correlation experiments (intra-residue $^{15}N_i$-($^{13}C\alpha^{13}C\beta)_i$ correlation and inter-residue $^{15}N_{i+1}$-($^{13}C\alpha^{13}C\beta)_i$ correlation) and ($^{13}C\alpha^{13}C\beta)_i$-($^{13}C\alpha^{13}C\beta)_{i+1}$ experiment were performed using reported pulse sequences [18]. The initial magnetization was prepared by cross polarization from the proton magnetization with a contact time of 2 ms and the RF field amplitude was ramped near the first sideband for the Hartmann–Hahn condition, $\gamma B^X{}_1 = \gamma B^H{}_1 - \omega_R$. Here, $\gamma B^X{}_1$ and $\gamma B^H{}_1$ are the RF field amplitudes of ^{13}C and ^{1}H respectively and ω_R is the sample spinning frequency. Frequency selective CP from ^{15}N to ^{13}C was used in ^{15}N–^{13}C correlation experiments [31,32]. Data matrix (512 (t1) × 1024 (t2), unless otherwise mentioned) was zerofilled to 1024 × 1024, multiplied by an exponential window function with a 100 Hz broadening factor, and analyzed with the aid of Felix version 2002 (Accelrys Inc., San Diego, CA USA). All two-dimensional spectra were presented by the contours with S/N > 3.0 except for otherwise specified. ^{13}C and ^{15}N chemical shift values were referenced to 2,2-dimethylsilapenatane-5-sulfonic acid (DSS) [33].

^{13}C NMR observation of $^{2}H/^{31}P$-selective ^{1}H-depolarization under magic angle spinning (COXSHD) was carried out at 11.74 T according to the reported method [34]. The RF phase for the depolarization period was alternated at the intervals of 240 and 160 μs for ^{2}H and ^{31}P, respectively. The ^{1}H depolarization was facilitated by the phase-alternating cross polarization. The flip angles of all the ^{1}H pulses are 54.7°. The B_1 field amplitudes satisfy the condition mentioned above at the spinning rate of 12.5 kHz. The $B^X{}_1$ amplitudes for ^{2}H and ^{31}P were 31 and 52 kHz, respectively. The frequency of $B^X{}_1$ was shifted by about 130 kHz under the off Hartmann–Hahn condition. Contact time for ^{13}C–^{1}H LGCP was 80 μs. The ^{1}H RF amplitude was 70 kHz. The 16,000 transients were accumulated at 193 K.

3. Results

3.1. Signal assignment of PC/PG-membrane bound PACAP21

Since PACAP21 did not bind to PC bilayers, DPPC/DPPG bilayers were used as membranes. To suppress the background signals from the lipids, deuterated DPPC-d_{62} and DPPG-d_{62} were used for sample preparation. The assignment of the signals was carried out as follows. At first, the type of amino acid was determined, using intra-residual ^{13}C,^{13}C- and ^{13}C,^{15}N- correlation spectra. The sequential number can be identified for single residues in the peptide at this stage. Then, the sequential assignment was performed using inter-residual $^{13}C_i$,$^{15}N_{i+1}$- and $^{13}C_i$,$^{13}C_{i+1}$-correlation 2D NMR spectra. Here, some of the signals were unequivocally assigned. Then, the overlapped

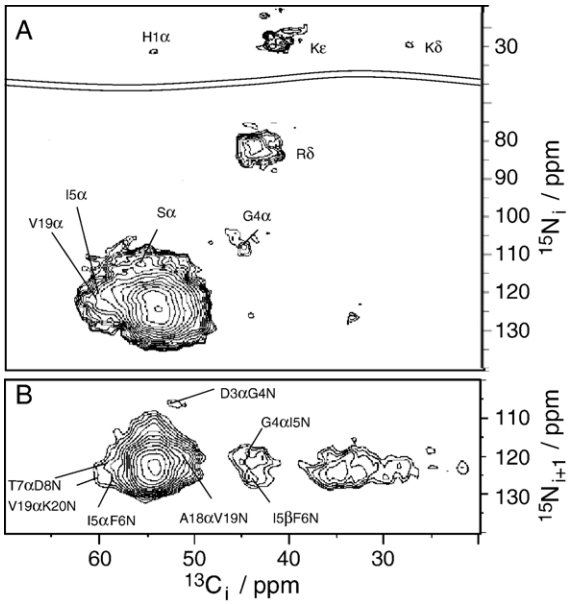

Fig. 2. 2D intra- and inter-residue ^{15}N–^{13}C correlation spectra of membrane-bound [U–^{13}C, ^{15}N] PACAP21 at 213 K. (A) Intra-residue ^{15}N–^{13}C correlation at 14.09 T. Contact time from N_i to C_i, 4 ms; number of acquisition, 64 for each FID; data matrix, 512 (t1) × 400 (t2); and ω_R = 16 kHz. (B) Inter-residue ^{15}N–^{13}C correlation at 11.74 T. Contact time from N_{i+1} to C'_i, 4 ms; DARR mixing time, 24 ms; number of acquisition, 60 for each FID; data matrix, 512 × 300; and ω_R = 12.5 kHz.

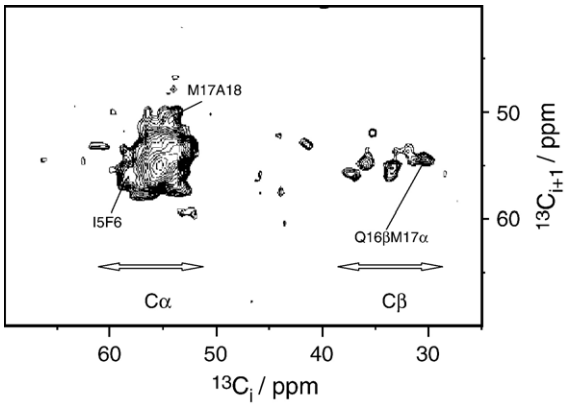

Fig. 3. A 2D inter-residue $(C\alpha C\beta)_i$–$C\alpha_{i+1}$ correlation spectrum of membrane-bound [U–^{13}C, ^{15}N] PACAP21 at 11.74 T and 213 K. Contact times from C_{i+1} to N_{i+1} and from N_{i+1} to C'_i, 2.5 and 4 ms, respectively; DARR mixing time, 24 ms; number of acquisition, 64 for each FID; and ω_R=12.5 kHz. The spectrum is composed of contours with S/N >2.3.

signals were tentatively assigned using bulk chemical shifts determined at the first step, assuming the presence of all signals.

A 2D homonuclear ^{13}C–^{13}C correlation DARR spectrum of the membrane-bound PACAP21 (lipid/peptide=36) is presented in Fig. 1. Assignment started with the BMRB database that gives the typical chemical shifts of amino acid residues. As shown in Fig. 1D, aliphatic carbon spin systems of Ile5, Thr7 and Val19 could be traced. Here, the numbered residues are uniquely assigned because they are single residues in PACAP21. Using the information from $^{13}C_i$,$^{15}N_i$-correlation in Fig. 2A, the spin systems of Arg and Lys were also traced. The Cα/Cβ cross peaks for Ala18 and Ser could be easily identified at (51, 23) and (56, 66) ppm. However, the signals of three Ser residues could not be observed separately. This is a typical feature of the spectra obtained in this work. We can get only bulk chemical shifts for each amino acid residue in an intra-residue correlation spectrum. The Cβ chemical shifts of Phe, Tyr and His were determined by Cβ/Cγ cross peaks (Fig. 1C). The Gly4 Cα/C', Ala18 Cβ/C' and Ser Cα/C' cross peaks could be also assigned in Fig. 1A. Signals at the lowest field could be assigned to the side chain carboxyl groups of Asp and carboxylamide groups of Gln16 and Lys21. Otherwise, the carbonyl signals were assumed to be located at overlapped peaks in Cβ/C' areas. This is reasonable because of their narrow distributions. The cross peaks of Cζ/Cδ, Cζ/Cγ, Cζ/Cβ and Cζ/Cα of Arg were identified at (160, 44), (160, 28), (160, 35) and (160, 54) ppm in a DARR spectrum with 200 ms mixing time as can be seen in Fig. 1B. There are contributions from Tyr to the signals at 44 and 54 ppm as well.

2D heteronuclear ^{15}N–^{13}C spectra for intra- and inter-residue correlations ($^{15}N_i$–$^{13}(C\alpha C\beta)_i$ and $^{15}N_{i+1}$–^{13}(CO, $C\alpha C\beta)_i$, respectively) are presented in Fig. 2. From the intra-residue correlation (Fig. 2A), Gly4 Cα/N, Lys Cε/NH_3^+, Lys Cδ/NH_3^+ and Arg Cδ/Nε cross peaks were identified as isolated peaks. Since His1 should have the terminal ammonium group, the cross peak at (^{15}N, ^{13}C)=(32, 55) ppm can be ascribed to His1 Cα/NH_3^+ correlation. On the basis of Cα chemical shifts determined and the general tendency of ^{15}N chemical shifts in BMRB, well-defined points in the overlapped signals are attributed to Ile5 Cα/N, Val19 Cα/N and Ser Cα/N, respectively. In the inter-residue correlation spectrum (Fig. 2B), D3CαG4N could be identified as an isolated peak. Possible assignments are also presented in the figure on the basis of the assignment of ^{13}Cα, namely, I5αF6N, T7αD8N, V19αK20N and A18αV19N in the major body of overlapping, and G4αI5N and I5βF8N in the neighbor.

A $C\alpha_{i+1}$–$(C\alpha C\beta)_i$ correlation spectrum of PACAP21 is shown in Fig. 3. We could assign well resolved $(C\alpha C\beta)_{i+1}$–$C\alpha_i$ cross peaks to I5αF6α and M17αA18α correlation signals on the basis of assigned chemical shifts for Ile5 Cα, Phe6 Cα and Ala18 Cα. Therefore, Met17 Cα/Cβ should be located in the congested region at around (54, 35) ppm. Since Cβ of Gln appears at the highest field except for that of Ala and the chemical shift of Met17Cα is known, the cross peak at (30, 54) ppm was attributed to Q16βM17α. Although the $C\alpha_{i+1}$–$C\alpha_i$ correlations for D3G4, G4I5, F6T7, A18V19 and V19K20 should appear as isolated or well-defined peaks, they failed to emerge. These cross peaks could not be observed even in lower contour levels. The assigned chemical shifts are summarized in Table 1. Signals only assigned to individual amino acids are shown in italics and the assignment of a signal overlapped with those of other amino acids is given in a parenthesis. The uncertainty due to the line-width is given for Cα, Cβ and C′ in the table.

Since we used a sample at a high peptide concentration, the effect of concentration on the chemical shifts was examined with a 10-fold diluted sample (lipid/peptide=360). 2D spectra could not be obtained with this sample. Thus, 1D MAS/CP ^{13}C-NMR spectra were recoded for the samples at high and low peptide concentrations. They are compared in Fig. 4. On

Table 1
Chemical shifts of ^{13}C and ^{15}N signals of membrane-bound PACAP21

a.a.	N^H	C′	Cα	Cβ	Cγ	Cδ	others
1H	32	[174±2]	55±1	32±1.3	131		
2S	*112*	*173±1.5*	*56±2*	*66±1.5*			
3D		[174±2]	53±2.5	45±2	*178*		
4G	108	171±2	45±1				
5I	120	[174±2]	59±1.5	42±1	29/18	14	
6F	126	[174±2]	56±2	44±2	133	[133]	ζ 128
7T		[174±2]	59.6±1.5	71±1.5	22		
8D	122	[174±2]	*53±2*	*45±2*	*178*		
9S	*112*	*173±1.5*	*56±2*	*66±1.5*			
10Y		[174±2]	[55±2.5]	*44±2*	*129*	[133]	*ε118/ζ158*
11S	*112*	*173±1.5*	*56±2*	*66±1.5*			
12R		[174±2]	[54±1.5]	*35±1.5*	*28*	*44*	*ζ160*/Nε*82*
13Y		[174±2]	[55±2.5]	*44±2*	*129*	[133]	*ε118/ζ158*
14R		[174±2]	[54±1.5]	*35±1.5*	*28*	*44*	*ζ160*/Nε82
15K		[174±2]	[54±1.5]	[36±1.5]	*26*	*29*	*ε42/Nζ30*
16Q		[174±2]	[54±1.5]	30±2	35	179	
17M		[174±2]	54±1	[35±*Δ]			
18A		175±1	51±1.3	23±1.5			
19V	122	[174±2]	60.4±1.5	35±2	22		
20K	126	[174±2]	[54±1.5]	[36±1.5]	*26*	*28*	*ε42/Nζ30*
21K		180±2	53±1.5	[36±1.5]	*26*	*28*	*ε42/Nζ30*

Italics, assignment to individual amino acid species; [ ], assignment for the signal overlapped with those of other amino acid species; *Δ=+2.5 and −4.

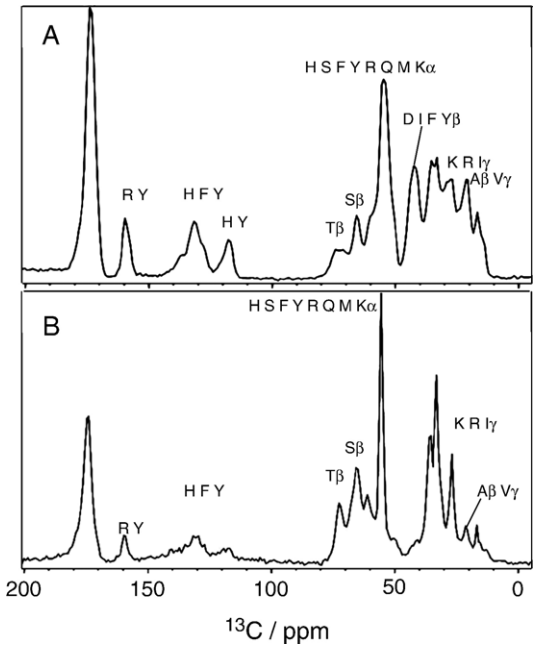

Fig. 4. Effect of peptide/lipid dilution on a 1D CP/MAS ^{13}C-NMR spectrum of membrane-bound [U–^{13}C, ^{15}N] PACAP21 at 11.74 T. (A) Peptide:lipid (mol/mol) = 1:36 at 233 K, and (B) the ratio = 1:360 at 223 K. The contact time, 2.2 ms for A and B; Number of acquisition, 960 and 52000 for A and B, respectively; and ω_R = 12.5 kHz. Possible amino acid residues contributing to each signal are given by single-letter codes.

dilution, the signals at around 71 ppm (Thr Cβ) became a singlet, and those at around 55 ppm got sharper. Furthermore, those at around 43 ppm are almost gone. The diminished signals did not recover even in the single pulse experiment under proton-decoupling, which might be ascribed to the interference between their motion and proton-decoupling. Although the reason of the spectral change is not yet clear at this stage, the chemical shifts of the observed signals did not change on dilution. It can be concluded that the major part of the membrane-bound peptide still takes on an extended conformation under the diluted condition.

3.2. Signal assignment of PC membrane-bound PACAP27

Since PACAP27 binds to DMPC bilayers, we prepared the sample with deuterated DMPC-d_{54}. This sample gave a better RFDR spectrum at 233 K and a better SPC-5 spectrum at 273 K. RFDR spectra gave the information essentially identical with that from SPC-5 spectra. ^{13}C–^{13}C correlation spectra of membrane-bound PACAP27 are presented in Fig. 5. The observed chemical shifts were the same within the resolution limits at temperature from 213 to 273 K. Under these conditions, the DMPC bilayers are in the gel state. In the double quantum dipolar mixing spectrum, one-step magnetization transfer gave rise to a negative intensity, colored green, and two-step magnetization transfer gave rise to a positive intensity, colored black. Spin connectivities of Ile, Thr, Val, Leu, and Arg could be traced as shown in the spectrum (Fig. 5C). Although there are two Leu Cα/Cβ cross peaks, they will be justified by later assignment. Those of Arg, Lys, and Gln16 also could be traced in the DARR spectrum (Fig. 5D). In the case of Arg and Lys, the chemical shifts determined by ^{13}C, ^{15}N-correlation (Fig. 6) were used. Cα/Cβ cross peaks of Ala and Ser were assigned from their characteristic chemical sifts. Although the intra-residue Cα/Cβ cross peaks of His, Arg, Lys and Met signals are overlapped,

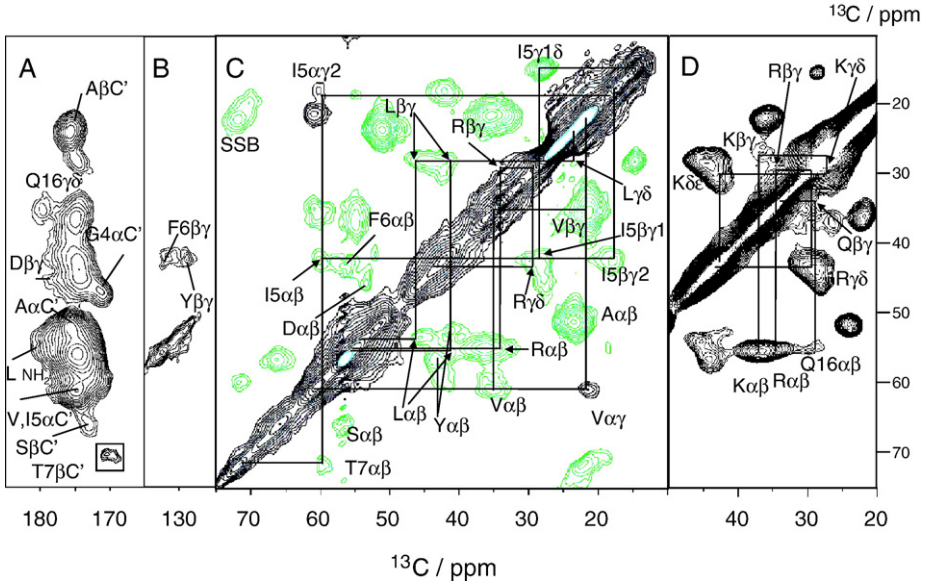

Fig. 5. 2D ^{13}C–^{13}C correlation spectra of membrane-bound [U–^{13}C, ^{15}N] PACAP27 at 16.44 T. (A) Aliphatic–carbonyl carbon correlation (DARR) at 233 K. Mixing time, 17 ms; number of acquisition, 64 for each FID; data matrix, 400 × 1024; and ω_R = 16 kHz. Sensitivity is enhanced in a squared region. (B) Aliphatic–aromatic carbon correlation (RFDR) at 233 K. Mixing time, 2.96 ms; number of acquisition, 16 for each FID; and ω_R = 13.5 kHz. (C) Aliphatic–aliphatic carbon correlation (SPC-5) at 273 K. Double quantum dipolar mixing time, 1.25 ms; number of acquisition, 64 for each FID; and ω_R = 16 kHz. The side-chain connectivity was indicated with solid lines. SSB stands for a spinning side band. (D) Aliphatic–aliphatic carbon correlation (DARR) at 233K. The parameters are same to those of A. The spectrum is presented by contours with S/N > 8.

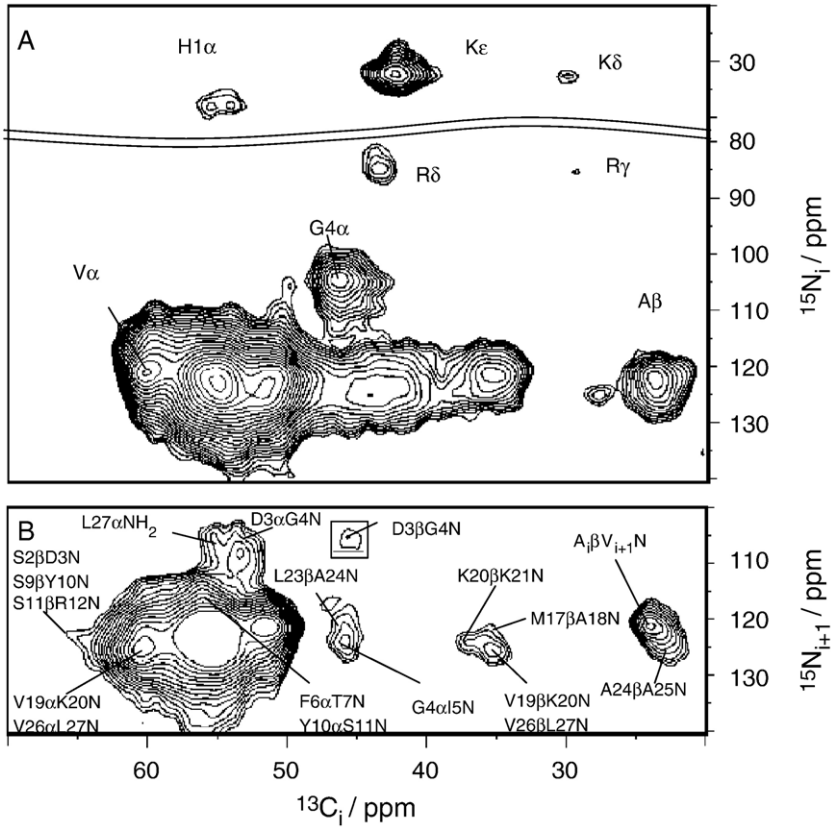

Fig. 6. 2D intra- and inter-residue ^{15}N–^{13}C correlation spectra of membrane-bound [U–^{13}C, ^{15}N] PACAP27 at 11.74 T and 273 K. (A) Intra-residue correlation. Contact time from N_i to C_i, 7 ms; number of acquisition, 64 for each FID; data matrix, 320×270; and ω_R=12.5 kHz. (B) Inter-residue correlation. Contact time from N_{i+1} to C'$_i$, 5 ms; RFDR mixing time, 2.24 ms; number of acquisition, 128 for each FID; data matrix, 320×400; and ω_R=12.5 kHz. Sensitivity is enhanced in a squared region.

some of their chemical shifts could be determined separately as will be described later. The Cβ chemical shifts of Phe, Tyr and His are determined using their Cβ/Cγ cross peaks (Fig. 5B). His1 Cβ/Cγ was very weak. In the case of Tyr, however, two Cα/Cβ cross peaks were assigned. At first, it was assigned to (56, 43) ppm from the major intensity of the Cβ/Cγ cross peak as in the case of Phe6. Since a weak cross peak at (53, 41) ppm was remained unassigned at the final stage of the assignment, this was tentatively assigned to Tyr in view of the Cβ chemical shift. In Fig. 5A, Gly4 Cα/C', Ala Cβ/C', Thr7 Cβ/C', Ser Cβ/C', Ile5 Cα/C' and Val Cα/C' could be assigned. Furthermore, signals at the lowest field could be assigned to the side chain carboxyl groups of Asp and carboxylamide groups of Gln16 and Leu27. Otherwise, the peak tops were interpreted as the overlapped carbonyl signals in Cβ/C' areas as in the case of PACAP21.

A 2D intra-residue ^{15}N–^{13}C correlation spectrum of PACAP27 is presented in Fig. 6A. The ^{15}N chemical shifts can be specified from the ^{13}C chemical shifts of isolated cross peaks. The His1 Cα/N, Gly4 Cα/N, Ala Cβ/N, Lys Cε/Nζ, Lys Cδ/Nζ, Arg Cδ/Nε and Arg Cγ/Nε cross peaks could be easily identified. His1 signal was observed as two peaks, suggesting that the N-terminus takes two conformations. On the basis of the carbon chemical shifts, Val Cα/N could be assigned as well. The inter-residue $^{15}N_{i+1}$–$^{13}(CO, C\alpha C\beta)_i$ correlation spectrum (Fig. 6B) provides more information. The cross peaks of D3Cα/G4N, D3Cβ/G4N and L27C'/NH_2 could be easily assigned because of well-distinguished ^{15}N chemical shifts. In the Ala cross peak, there are evidently two kinds of signals, which were assigned to two $A_iC\beta/V_{i+1}N$ and A24Cβ/A25N, respectively, on the basis of their intensity. Otherwise, indicated in the spectrum are the cross peaks that were assigned on the basis of carbon and nitrogen chemical shifts so far obtained.

A $C\alpha_{i+1}$–$C\alpha_i$ correlation spectrum of the membrane-bound PACAP27 shown in Fig. 7 provided further information for Cα. In contrast to PACAP21, isolated and peripheral cross peaks are well defined except for D3G4. Thus, we can make a sequential walking using the chemical shifts assigned so far. In the N-terminal region, the walking starts from well-defined cross peaks, namely, G4/I5, F6/T7, and T7/D8. I5/F6 can be identified from G4/I5 and F6/T7. Since we know the chemical shifts of His1 and Asp3, the walking can be extended to the N-terminus by use of the bulk chemical shift of Ser. The cross peak M17/A18 can be assigned on the basis of Ala chemical shift as in the case of PACAP21. Since the chemical shift of Gln16 is known, we can walk from Gln16 to the C-terminus on the basis of the well-defined cross-peaks, A18/V19, V19/K20, L23/A24, A24/A25, A25/V26, and V26/L27, provided that the chemical shifts of Lys21 and Tyr22 are known. Note that the chemical shifts of Lys20 and Ala25 are different from the bulk value of

each amino acid residue, respectively. There are two possibilities for Tyr22, namely, 53 and 56 ppm. In the case of the former, Y22/L23 should appear on the diagonal line. Since there is no signal intensity in the expected region in Fig. 7, the chemical shift of Tyr22 was assigned to 56 ppm. The bulk shift (55 ppm) was used for Lys21. From Ser9 to Lys15, the walking was carried out using bulk chemical shifts of Ser, Lys and Arg because of serious overlapping of the cross peaks. There are two possibilities for Tyr residues as in the case of Tyr22. If Tyr10 is assigned to 53 ppm, the intensity in the central region cannot be explained. In contrast, Tyr13 fits to 53 ppm. Therefore, Tyr10 and Tyr13 are assigned to 56 and 53 ppm, respectively. Now, the walking from the N- to C-termini is accomplished. This walking not only confirm the observed chemical shifts, but also provided more exact chemical shifts for some signals. Assigned chemical shifts of PACAP27 are summarized in Table 2 in the same way as for PACAP21.

3.3. Selective polarization transfer from PACAP to membranes

To confirm the binding of the PACAP peptide to phospholipid membranes, the polarization transfer from the proton spins of the PACAP27 to $^{2}H/^{31}P$ one of membranes was measured. COXSHD spectra of the membrane-bound PACAP27 for $^{1}H–^{31}P$ and $^{1}H–^{2}H$ transfer are presented in Fig. 8A and B, respectively. To make the cross polarization efficient, the measurement was carried out at 193 K. In Fig. 8A, the polarization transfer was observed for Tyr, Phe, His, Ser Cβ, Thr Cβ, some of Cα and side chains of Ile, Leu, Asp, Lys and Arg. This reveals that PACAP27 actually binds to phospholipid bilayers. Since phosphate groups are located on the surface of phospholipid membranes, the peptide should lay on the membrane surface. The polarization transfer from the protons to the deuterons of fatty acids provides the information about the amino acid residues interacting with the hydrophobic region of the membrane. In Fig. 8B, the transfer was also observed for aliphatic carbons and aromatic carbons. However, the pattern is different from that in Fig. 8A. Especially, the transfer was mainly observed for Phe in the aromatic region, judged from the weak HY signal. This indicates that the side chain of Phe is inserted into the hydrophobic region, while those of His and Tyr stay in the surface region. In the aliphatic region, the polarization was observed mainly for Cβ and Cγ of Ile, Leu and Val, and Cβ of Ala and Phe. This fact shows that PACAP27 is localized on the membrane surface with the hydrophobic side chains being inserted into the inner region of the membrane. Since Ala, Leu and Val are the residues in the C-terminal region of PACAP27, the C-terminal hydrophobic region plays an important role in binding to the membrane.

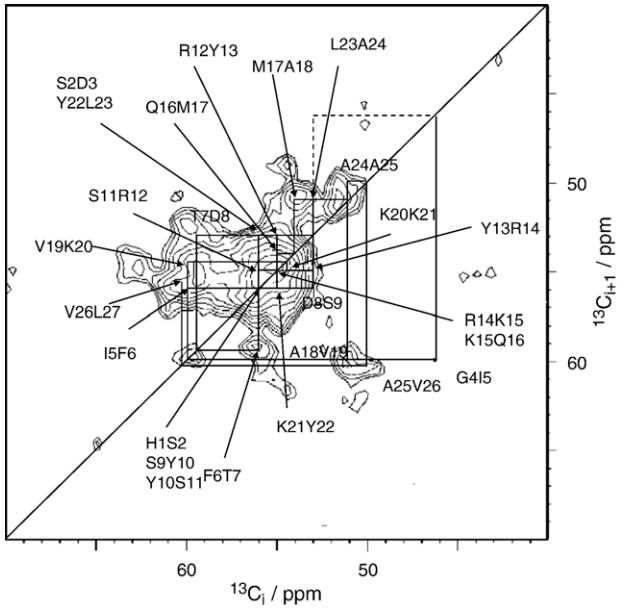

Fig. 7. A 2D $^{13}C\alpha_i–^{13}C\alpha_{i+1}$ correlation spectrum of membrane-bound [U–^{13}C, ^{15}N] PACAP27 at 11.74 T and 213 K. Contact times from $C\alpha_{i+1}$ to N_{i+1} and from N_{i+1} to C'_i, 2.5 and 4 ms, respectively; DARR mixing time, 24 ms; number of acquisition, 64 for each FID; data matrix, 400×1024; and ω_R=12.5 kHz. Sequential assignment of Cα is indicated by solid lines. The dashed line shows the connection of D3G4. The spectrum is composed of contours with S/N >2.3.

Table 2
Chemical shifts of ^{13}C and ^{15}N signals of membrane-bound PACAP27

a.a.	N^H	C'	Cα	Cβ	Cγ	Cδ	Others
1H	38	[174±2]	55.6/54±1.5	30±1	*130*		
2S		*173±1.5*	*56±1.5*	*66±2*			
3D	122	[174±2]	53±1.5	46±2	*178*		
4G	105	171±1	46±1.5				
5I	[124]	[175±1.7]	59.5±1	42±2	28/18	15	
6F	[122]	[174±2]	56±2.5	43±1.5	133	[132]	ζ 130
7T	112	170±1	59.5±1	72±1	19.5		
8D		[174±2]	*53±1.5*	*46±2*	178		
9S		*173±1.5*	*56±1.5*	*66±2*			
10Y	[122]	[174±2]	*56±1.5*	*43±2*	*129*	[132]	*ε117/ζ158*
11S	[115]	*173±1.5*	*56±1.5*	*66±2*			
12R	[122]	[174±2]	[55±1.5]	*34±2*	*29.5*	*43.5*	*ζ160*/Nε*85*
13Y		[174±2]	53±1.5	41±1.5	*129*	[132]	*ε117/ζ158*
14R		[174±2]	[55±1.5]	*34±2*	*29.5*	*43.5*	*ζ160*/Nε*85*
15K		[174±2]	[55±1.5]	*36±2*	*27*	*30*	*ε42*/Nζ*32*
16Q		[174±2]	55±1.3	29±2	35	179	
17M		[174±2]	54±1.5	[35±2]			
18A	122	*175.6±1*	51±1.5	*24±1.5*			
19V	[120]	[175±1.7]	59.5±1	*35±1.5*	21		
20K	[125]	[174±2]	54.5±2	37±1	*27*	*30*	*ε42*/Nζ*32*
21K	[125]	[174±2]	[55±2]	*36±2*	*27*	*30*	*ε42*/Nζ*32*
22Y		[174±2]	[56±1.5]	*43±2*	*129*	[132]	*ε117/ζ158*
23L		[174±2]	53±2	46±2	28		
24A	122	*175.6±1*	51±1.5	23±1.5			
25A	125	*175.6±1*	50±1.5	*24±1.5*			
26V	[120]	[175±1.7]	60±1	*35±1.5*	21		
27L	[125]	181±2	55±2	41±1.5	28		NH_2 107

Italics, assignment to individual amino acid species; [ ], assignment for the signal overlapped with those of other amino acid species.

4. Discussion

4.1. Secondary structural analysis of PACAP21 and PACAP27

The spectral sensitivity and resolution was better for PACAP27 than for PACAP21, which may be attributed to differences in the phospholipid composition and the rotor size. Because of broad line-widths, the sequentially assigned signals were 10/21Cα, 8/20Cβ and 3/21C' for PACAP21, and 17/27Cα,

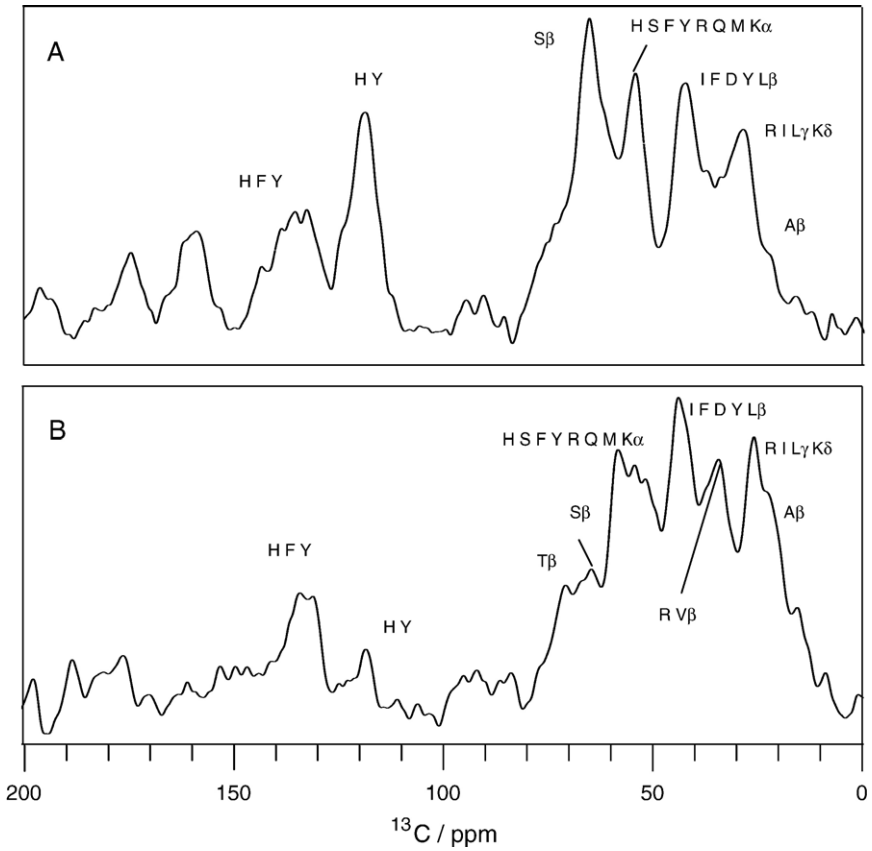

Fig. 8. 1D $^{31}P/^{2}H$-selective ^{1}H-depolarization ^{13}C-NMR (COXSHD) spectra of membrane-bound [U–^{13}C, ^{15}N] PACAP27. (A) ^{31}P–^{1}H–^{13}C polarization transfer, and (B) ^{2}H–^{1}H–^{13}C polarization transfer. Amino acid residues which may contribute to each signal are indicated by single-letter codes.

11/26Cβ and 3/27C' for PACAP27. However, the uncertainty was within±2 ppm for most signals. For isolated peaks of single residues, the line-width is 2–3 ppm. Since the contribution of line-broadening factor is 0.8 ppm, the intrinsic line-width should be 1.2–2.2 ppm. The ^{13}C linewidth of 1.5–2 ppm at 11.74 was reported to be a typically well-structured and rigid non-crystalline peptide, while a disordered structure gives a 4–5 ppm [35]. Therefore, PACAP21 and PACAP27 should take a relatively well-defined structure.

We have calculated the main chain φ and ψ angles with the program TALOS version 2003.027.13.05, using $^{13}C\alpha$, $^{13}C\beta$, and $^{13}C'$ chemical shifts [36]. Predicted φ and ψ angles are plotted in red in Fig. 9. The classification was "good" for all residues except Gly4. In view of the broad line-widths, the effect of the uncertainty on the prediction of dihedral angles was checked. The dihedral angles were calculated for the chemical shifts $\delta\alpha_i+\Delta\delta\alpha_i$ and $\delta\beta_i-\Delta\delta\beta_i$, where Δδ is the uncertainty shown in Tables 1 and 2. This gives the largest change favorable for a helical conformation. Nevertheless, the obtained angles are favorable for extended conformations in spite of two unreliable angle pairs (Fig. 9, in green). Calculations for the chemical shifts $\delta\alpha_i-\Delta\delta\alpha_i$ and $\delta\beta_i+\Delta\delta\beta_i$ were also carried out, which gave the angles favorable for extended conformations (Fig. 9, in blue). This result indicates that backbone dihedral angles of membrane-bound PACAP21 and PACAP27 fit to extended conformations. Then, the chemical shifts were calculated for all extended conformations with SHIFTX. They matched the observed chemical shifts except Gly4. Therefore, we have concluded that both PACAP21 and PACAP27 take on the extended conformation on binding to lipid membranes in the gel state, although there could be a distortion around Gly4.

4.2. Comparison of the obtained conformations with those of PACAP27 in micelles and PACAP21 bound to the receptor

The reported structure of the DPC micelle-bound PACAP27 comprises a long α-helix (residues 5–27) flanked by a disordered N-terminal tail (residues 1–4) [16]. This is different from the extended conformation of the membrane-bound PACAP27 determined in this work. Therefore, carbon chemical shifts were calculated with SHIFTX [37] for all α-helix structure of PACAP27 and mapped on a ^{13}C–^{13}C correlation spectrum of DMPC membrane-bound PACAP27. The calculated cross peaks did not match the observed one (data not shown), confirming that the secondary structure of membrane-bound PACAP27 is different from the conformation in DPC micelles.

A 2D ^{13}C–^{13}C DARR spectrum of PACAP21 with a mixing time 500 ms was observed to detect relatively long-range distances (~6.5 Å). It is presented in Fig. 10. A well-separated peak at (46, 60) ppm could be assigned to either G4Cα/T7Cα or G4Cα/V19Cα correlation. One possibility is that G4T7 correlation is caused by bending of peptide as in the case of the receptor-bound PACAP21 [16]. However, the predicted dihedral angles in Fig. 9 contradict this idea. So, this correlation

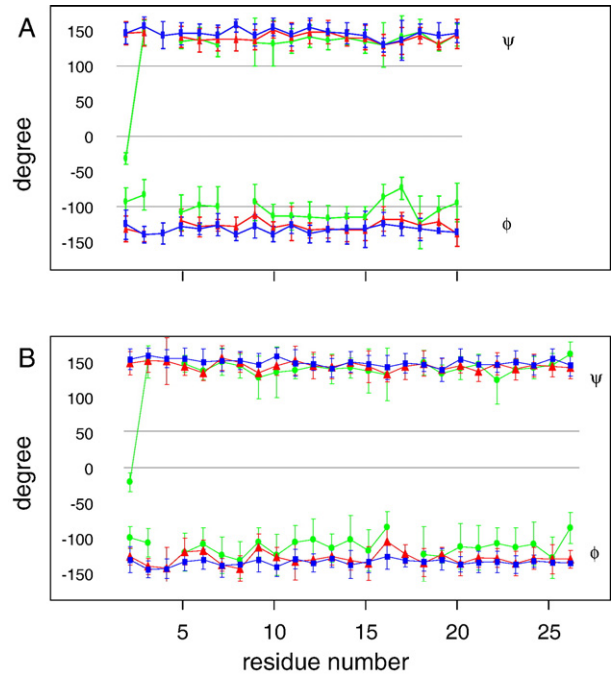

Fig. 9. Backbone dihedral angles ϕ and ψ predicted with TALOS as a function of residue number. (A), PACAP21; (B), PACAP27. The chemical shifts of Cα, Cβ and C' in Tables 1 and 2 were used for calculation. Symbols; red triangle, for observed chemical shifts (δ_i); green circle, for $\delta\alpha_i+\Delta\delta\alpha_i$ and $\delta\beta_i-\Delta\delta\beta_i$; and blue square, for $\delta\alpha_i-\Delta\delta\alpha_i$ and $\delta\beta_i+\Delta\delta\beta_i$. The error bars indicate RMSD for the predicted dihedral angles. Angles with less than 7 reliable pairs are omitted.

should be originated from the inter-chain distance. If the peptide region of His1–Tyr10 takes on an antiparallel β-sheet that brings Gly4 and Thr7 close to each other, Asp3 and Asp8 line up side by side. This would be unstable on the membranes with net negative charges. Therefore, a possible structure is an antiparallel β-sheet formed by the peptide region from Ser2 to Lys21 that brings Gly4 and Val19 close to each other.

4.3. Conformational characteristics of PACAP27 and PACAP21 bound to the membranes

Although the overall conformation is the same for PACAP21 and PACAP27, the binding mechanism is different. While the former cannot bind to PC membranes, the latter can. The side chains of the hydrophobic residues of PACAP27 were shown to be involved in the binding. Therefore, the nature of the binding for the former and latter should be electrostatic and hydrophobic interactions, respectively. In the measurement of $C\alpha_{i+1}$–$(C\alpha C\beta)_i$ correlation of PACAP21, the cross peaks of D3G4, G4I5, F6T7, A18V19 and V19K20 could not be observed in the expected regions. Although we do not have the information on H1S2 and S2D3 because of their localization in the congested region, it is strongly suggested that the N-terminal region is relatively flexible even at 223 K because of the soft interaction on the membrane surface. Since the pulse sequence of the $C\alpha_{i+1}$–$(C\alpha C\beta)_i$ correlation includes three cross polarizations, mobility makes the total polarization transfer inefficient. Since D3G4 cross peak could not be observed and the intensity of G4I5 was very weak, the N-terminal region (His1–Ile5) seems to be flexible also for PACAP27. The extended structures for PACAP21 and PACAP27 reveal that it cannot be ascribed to the nature of peptide–membrane interactions. Furthermore, the dilution of PACAP21 did not change the extended conformation as shown above. The sharp signals strongly suggest that the peptide takes on a well-defined structure in monomers or small oligomers, showing that a high concentration of the peptide is not responsible for the extended structure formation. Therefore, it can be concluded that the interaction of PACAP peptides with the membrane surface causes their extended conformation, which should be ascribed to its amino acid sequence.

A possible origin of the extended conformations for PACAP21 and PACAP27 is fibril formation induced by lipid bilayers. The fibril formation usually needs a certain time for nucleation and elongation. In the case of monosialoganglioside GM1-induced fibril formation, it took 12–20 h [38]. However, PACAP21 and PACAP27 bind liposomes instantly. Furthermore, a dilution of the peptide did not change the conformation. Therefore, a huge fibril formation is not likely, although a short fibril formation on the membrane cannot be eliminated at this stage. Furthermore, we cannot rule out the possibility that PACAP becomes a monomer only at very low concentration, and the monomer takes on an α-helical conformation.

4.4. Biological significance of the variable conformation for PACAP27

The structure of micelle-bound PACAP27 comprises a long α-helix (residues 5–27) and a disordered N-terminal tail (residues 1–4) [16]. In the case of the receptor-bound PACAP21 structure, however, there are an extended N-terminal tail (residues 1–2), a consecutive β-turns (residues 3–7) and an α-helix (residues 8–21) [16]. An N-terminally truncated PACAP38 (residues 6–38) takes on α-helix in the receptor [17]. In these cases, the α-helix is the major secondary structure. Therefore, this peptide changes its conformation depending on its environment or interacting partners. Usually, a conformation in micelles is also realized in membranes. However, this is not

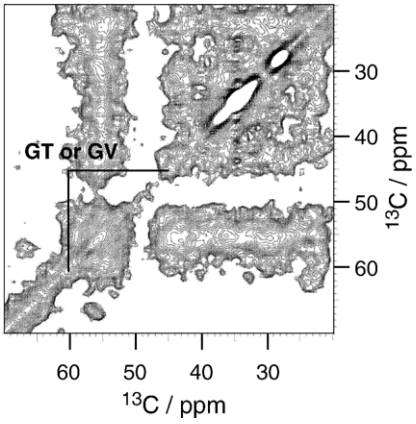

Fig. 10. A 2D ^{13}C–^{13}C correlation DARR spectrum of membrane-bound [U–^{13}C, ^{15}N] PACAP21 at 11.74 T and at 233 K. Mixing time, 500 ms; number of acquisition, 64 for each FID; data matrix, 400×1024; and ω_R=12.5 kHz.

the case with PACAP27. Furthermore, many of membrane-bound peptides reported so far take on α-helices [19,21]. This is also not the case with PACAP27. Therefore, we can conclude that this hormone peptide has a unique conformational property. A conformational change on membranes was suggested for fusogenic peptide B18, related viral fusogenic peptides [39] and an amyloid precursor protein Aβ(1–40) [38,40]. B18 takes on α-helix under lipid/peptide >100, and β-sheets at a higher peptide concentration, which induce membrane-fusion. Aβ(1–40) takes on helix-rich conformations when it binds to monosialoganglioside GM1 bilayers, then forms amyloid fibrils after 12–20 h. These are also the examples that peptides can change their conformations depending on their environments.

It has been indicated that the N-terminal residues are important for the receptor recognition and C-terminal residues facilitate the binding ability. Actually, the deletion of His1–Ile5 caused 200-fold reduction in the binding affinity [41]. The N-terminal regions of both PACAP27 and PACAP21 were shown flexible even on the membrane surface in this work. In contrast, the C-terminal region of PACAP27 was shown to be involved in the membrane binding in the polarization transfer experiment. These properties would be important for PACAP27 to bind the receptor and exert an induced fit on it, provided that membranes are involved in the receptor binding. PACAP27 is known to work in various sites in a wide variety of tissues. Its conformational flexibility may be associated with the variable roles in different places. Actually, an N-terminally truncated neurotensin (residues 8–13) was reported to take on a β-strand in its G-protein coupled receptor bound form [42].

Acknowledgments

We are grateful to Prof. Takahisa Ikegami (Osaka University) and Dr. Takeshi Tenno (Kyoto University) for their valuable discussions. This work was partly supported by Grants-in-Aid for Scientific Research on Priority Areas from the Ministry of Education, Science, Technology, Sport and Culture of Japan (HA and MS), and grants from JST (Target Protein Project) (HA and TF).

References

[1] S. Ohkubo, C. Kimura, K. Ogi, K. Okazaki, M. Hosoya, H. Onda, A. Miyata, A. Arimura, M. Fujino, Primary structure and characterization of the precursor to human pituitary adenylate cyclase activating polypeptide, DNA Cell Biol. 11 (1992) 21–30.

[2] A. Miyata, A. Arimura, R.R. Dahl, U. Minamino, A. Uehara, L. Jiang, M.D. Culler, D.H. Coy, Isolation of a novel 38 residue hypothalamic polypeptide which stimulates adenylate cyclase in pituitary cells, Biochem. Biophys. Res. Commun. 164 (1989) 567–574.

[3] K. Ogi, C. Kimura, H. Onda, A. Arimura, M. Fujino, Biochem. Biophys. Res. Commun. 166 (1990) 81–89.

[4] K. Okazaki, Y. Itoh, K. Ogi, S. Ohkubo, H. Onda, A novel peptide which stimulates adenylate cyclase: molecular cloning and characterization of the ovine and human cDNAs, Peptides 16 (1995) 1295–1299.

[5] J.E. McRory, R.L. Parker, N.M. Sherwood, Expression and alternative processing of a chicken gene encoding both growth hormone-releasing hormone (GRF) and pituitary adenylate cyclase-activating polypeptide (PACAP), DNA Cell Biol. 16 (1997) 95–102.

[6] N. Chartrel, M.C. Tonon, H. Vaudry, J.M. Conlon, Primary structure of frog pituitary adenylate cyclase activating polypeptide. (PACAP) and effects of ovine PACAP on frog pituitary, Endocrinology 129 (1991) 3367–3371.

[7] D.B. Parker, I.R. Coe, G.H. Dixon, N.M. Sherwood, Two salmon neuropeptides encoded by one brain cDNA are structurally related to members of the glucagon superfamily, Eur. J. Biochem. 215 (1993) , 439–448.

[8] J.E. McRory, D.B. Parker, S. Ngamvongchon, N.M. Sherwood, Sequence and expression of cDNA for pituitary adenylate cyclase activating polypeptide (PACAP) and growth hormone-releasing hormone (GHRH)-like peptide in catfish, Mol. Cell. Endocrinol. 108 (1995) 169–177.

[9] J.E. McRory, N.M. Sherwood, Pituitary adenylate cyclase activating polypeptide and related family members, Endocrinology 138 (1997) 2380–2390.

[10] A. Arimura, Perspectives on pituitary adenylate cyclase activating polypeptide (PACAP) in the neuroendocrine, endocrine, and nervous systems, Jpn. J. Physiol. 48 (1998) 301–331.

[11] D. Vaudry, B.J. Gonzalez, M. Basille, L. Yon, A. Fournier, H. Vaudry, Pituitary adenylate cyclase activating polypeptide and its receptors: from structure to functions, Pharmacol. Rev. 52 (2000) 69–324.

[12] K. Tornoe, J. Hannibal, T.B. Jensen, B. Georg, L.F. Rickelt, M.B. Andreasen, J. Fahrenkrug, J.J. Holst, PACAP-(1–38) as neurotransmitter in the porcine adrenal glands, Am. J. Physiol: Endocrinol. Metab. 279 (2000) 1413–1425.

[13] Y. Ishizuka, K. Kashimoto, V. Mochizuki, K. Sato, K. Ohshima, N. Yanaihara, Cardiovascular and respiratory actions of pituitary adenylate cyclase-activating Polypeptides, Regul. Pept. 40 (1992) 29–39.

[14] B.R. Steenstrup, B. Ottesen, M. Jorgensen, J.C. Jorgensen, Pituitary adenylate cyclase-activating polypeptide induces vascular relaxation and inhibits nonvascular smooth muscle activity in the rabbit female genital tract, Acta Physiol. Scand. 152 (1994) 129–136.

[15] T. Yada, M. Sakurada, K. Ihida, M. Nakata, F. Murara, A. Arimura, M. Kikuchi, Pituitary adenylate cyclase-activating polypeptide is an extraordinarily potent intra-pancreatic regulator of insulin secretion from islet β-cells, J. Biol. Chem. 269 (1994) 1290–1293.

[16] H. Inooka, T. Ohtaki, O. Kitahara, T. Ikegami, S. Endo, C. Kitada, K. Ogi, H. Onda, M. Fujino, M. Shirakawa, Conformation of a peptide ligand bound to its G-protein coupled receptor, Nat. Struct. Biol. 8 (2001) 161–165.

[17] S. Chaohong, S. Danying, A.D. Rachel, L.W. Barrett, V.E. Scott, P.L. Richardson, A. Pereda-Lopez, M.E. Uchic, L.R. Solomon, M.R. Lake, K.A. Walter, P.J. Hajduk, T. Olejniczak, Solution structure and mutational analysis of pituitary adenylate cyclase-activating polypeptide binding to the extracellular domain of PAC1-RS, Proc. Natl. Acad. Sci. U. S. A. 104 (2007) 7875–7880.

[18] T. Fujiwara, Y. Todokoro, H. Yanagishita, M. Tawarayama, T. Kohno, K. Wakamatsu, H. Akutsu, Signal assignments and chemical-shift structural analysis of uniformly ^{13}C, ^{15}N-labeled peptide, mastoparan-X, by mutidimentional solid-state NMR under magic-angle spinning, J. Biomol. NMR 28 (2004) 311–325.

[19] Y. Todokoro, I. Yumen, K. Fukushima, S.W. Kang, J.S. Park, T. Kohno, K. Wakamatsu, H. Akutsu, T. Fujiwara, Structure of tightly membrane-bound mastoparan-X, a G-protein-activating peptide, determined by solid-state NMR, Biophys. J. 91 (2006) 1368–1379.

[20] M. Kobayashi, Y. Matsuki, I. Yumen, T. Fujiwara, H. Akutsu, Signal assignments and chemical-shift structural analysis of uniformly [^{13}C, ^{15}N]-labeled membrane protein, H+-ATP synthase subunit c, by magic angle spinning solid state NMR, J. Biomol. NMR 36 (2006) 279–293.

[21] A. Ramamoothy (Ed.), NMR spectroscopy of biological solids, CRC Press, New York, 2006.

[22] T. Tenno, N. Goda, Y. Tateishi, H. Tochio, M. Mishima, H. Hayashi, M. Shirakawa, H. Hiroak, High-throughput construction method for expression vector of peptides for NMR study suited for isotopic labeling, Protein Eng. Des. Sel. 17 (2004) 305–314.

[23] B.A. Eipper, S.L. Milgram, E.J. Husten, H.Y. Yun, R.E. Mains, Peptidylglycine alpha-amidating monooxygenase a multifunctional protein with catalytic, processing, and routing domains, Protein Sci. 2 (1993) 489–497.

[24] A.E. Bennett, C.M. Rienstra, M. Auger, K.V. Lakshmi, R.G. Griffin, Heteronuclear decoupling in rotating solids, J. Chem. Phys. 103 (1995) 6951–6958.
[25] V. Ladizhansky, E. Vinogradov, B.J. van Rossum, H.J.M. de Groot, S. Vega, Multiple-spin effects in fast magic angle spinning Lee–Goldburg cross-polarization experiments in uniformly labeled compounds, J. Chem. Phys. 118 (2003) 5547–5557.
[26] A.E. Bennett, C.M. Rienstr, J.M. Griffiths, W.G. Zhen, P.T. Lansbury, R.G. Griffin, Homonuclear radio frequency-driven recoupling in rotating solids, J. Chem. Phys. 108 (1998) 9463–9479.
[27] A.E. Bennett, J.H. Ok, R.G. Griffin, S. Vega, Chemical-shift correlation spectroscopy in rotating solids: radio frequency-driven dipolar recoupling and longitudinal exchange, J. Chem. Phys. 96 (1992) 8624–8627.
[28] M. Hohwy, C.M. Rienstra, C.P. Jaroniec, R.G. Griffin, Fivefold. symmetric homonuclear dipolar recoupling in rotating solids: application to double. quantum spectroscopy, J. Chem. Phys. 110 (1999) 7983–7992.
[29] K. Takegoshi, S. Nakamura, T. Terao, ^{13}C–^{1}H dipolar-assisted rotational resonance in magic-angle spinning NMR, Chem. Phys. Lett. 344 (2001) 631–637.
[30] K. Takegoshi, T. Terao, ^{13}C nuclear Overhauser polarization nuclear magnetic resonance in rotating solids: replacement of cross polarization in uniformly ^{13}C labeled molecules with methyl groups, J. Chem. Phys. 117 (2002) 1700–1707.
[31] M. Baldus, A.T. Petkova, J. Herzfeld, R.G. Griffin, Cross polarization in the tilted frame: assignment and spectral simplification in heteronuclear spin systems, Mol. Phys. 95 (1998) 1197–1207.
[32] A.T. Petkova, M. Baldus, M. Belenky, M. Hong, J. Herzfeld, R.G. Griffin, Backbone and sidechain assignment strategies for multiply labeled membrane peptides and proteins, J. Magn. Reson. 160 (2003) 1–12.
[33] W.L. Earl, D.L. VanderHart, Measurement of ^{13}C chemical shifts in solids, J. Magn. Reson. 48 (1982) 35–54.
[34] E. Harada, Y. Todokoro, H. Akutsu, T. Fujiwara, Detection of peptide–phospholipid interaction sites in bilayer membranes by ^{13}C NMR spectroscopy: observation of ^{2}H,^{31}P-selective ^{1}H-depolarization under magic-angle spinning, J. Am. Chem. Soc. 128 (2006) 10654–10655.
[35] A.T. Petkova, Y. Ishii, J.J. Balbach, O.N. Antzutkin, R.D. Leapman, F. Delaglio, R. Tycko, A structural model for Alzheimer's-amyloid fibrils based on experimental constraints from solid state NMR, Proc. Natl. Acad. Sci. U. S. A. 99 (2002) 16742–16747.
[36] G. Cornilescu, F. Delaglio, A. Bax, Protein backbone angle restraints from searching a database for chemical shift and sequence homology, J. Biomol. NMR 13 (1999) 89–302.
[37] D.S. Wishart, B.D. Sykes, F.M. Richards, Relationship between nuclear magnetic resonance chemical shift and protein secondary structure, J. Mol. Biol. 222 (1991) 311–333.
[38] T. Okada, M. Wakabayashi, K. Ikeda, K. Matsuzaki, Formation of toxic fibrils of Alzheimer's amyloid β-protein-(1–40) by monosialoganglioside GM1, a neuronal membrane component, J. Mol. Biol. 371 (2007) 481–489.
[39] S.L. Grage, S. Afonin, M. Grün, A.S. Ulrich, Interaction of the fusogenic peptide B18 in its amiloyd state with lipid membrane studied by solid-state NMR, Chem. Phys. Lipids 32 (2004) 65–77.
[40] K. Matsuzaki, Physicochemical interactions of amyloid b-peptide with lipid bilayers, Biochim. Biophys. Acta 1768 (2007) 1935–1942.
[41] P. Robberecht, P. Gourlet, P. de Neef, M.C. Woussen-Colle, M.C. Piret, A. Vandermeers, J. Christophe, Structural requirements for the occupancy of pituitary adenylate-cyclase-activatingpeptide (PACAP) receptors and adenylate cyclase activation in human neuroblastoma NB-OK-1 cell membranes: discovery of PACAP (6–38) as a potent antagonist, Eur. J. Biochem. 207 (1992) 239–246.
[42] S. Luca, J.F. White, A.S. Sohal, D.V. Fillippov, J.H. van Boom, R. Grisshammer, M. Baldus, The conformation of neurotensin bound to its G-protein-coupled receptor, Proc. Natl. Acad. Sci. U. S. A. 100 (2003) 10706–10711.